



Electrochemistry of stainless steel colonized by manganese-oxidizing bacteria
by Wayne Harold Dickinson

A thesis submitted in partial fulfillment of the requirements for the degree of Doctor of Philosophy in
Chemistry

Montana State University

© Copyright by Wayne Harold Dickinson (1996)

Abstract:

Microbial colonization of stainless steel (SS) surfaces can modify the electrochemical properties of the metal and increase the risk of corrosion damage. Two dominant effects of colonization -a several hundred millivolt noble shift in electrical potential and a two to three decade increase in cathodic current density- are implicated in the corrosion processes. These effects, collectively known as Ennoblement, are attributed to the metabolic activity of attached microorganisms, however the mechanism by which microbial activity modifies cathodic reactions at the metal surface remains unclear. The present dissertation investigates the role of microbially generated oxidants in Ennoblement and demonstrates that Ennoblement is caused by manganic oxide biomineralization.

Microelectrode measurements of dissolved oxidants within biofilms on SS indicated that redox potential in the bulk biofilm did not change during Ennoblement. A proposed mechanism involving oxygen electroreduction was also eliminated by showing that cathodic rates were independent of oxygen concentration. The findings directed attention to microbial production of surface-bound oxidants. Quantification of metal capacitance and surface-bound reactants suggested that metal oxides were involved in Ennoblement and led to the hypothesis that Ennoblement is caused by manganic oxide biodeposition.

Epifluorescence microscopy and bacterial culture methods confirmed the presence of manganese-oxidizing bacteria on Ennobled SS. Manganese-rich surface deposits were confirmed by wet chemical and energy-dispersive x-ray analysis. SS coated with MnO₂ paste exhibited electrochemical properties that closely matched those of Ennobled SS and elevated electrical potential decayed to pre-exposure values when bisulfite ion was used to reductively dissolve the surface manganese deposits. The biological mechanism of Ennoblement was validated by inducing the effect using pure cultures of the manganese-oxidizing bacterium *Leptothrix discophora*. Coulometric titration and wet chemical analysis demonstrated that 15-75 nmoles cm⁻² of manganic oxide surface deposit shifts the potential of SS to a value near +350 mV versus the saturated calomel electrode.

Manganese-oxidizing bacteria have been widely reported at sites of SS corrosion. The present dissertation unifies this observation with the separate issue of Ennoblement by linking both issues to a common cause, manganic oxide biomineralization. The finding provides a plausible explanation for the corrosive effects of manganese-oxidizing bacteria on SS.

ELECTROCHEMISTRY OF STAINLESS STEEL COLONIZED BY
MANGANESE-OXIDIZING BACTERIA

by

Wayne Harold Dickinson

A thesis submitted in partial fulfillment
of the requirements for the degree

of

Doctor of Philosophy

in

Chemistry

MONTANA STATE UNIVERSITY-BOZEMAN
Bozeman, Montana

November 1996

D378
D5602

APPROVAL

of a thesis submitted by

Wayne Harold Dickinson

This thesis has been read by each member of the thesis committee and has been found to be satisfactory regarding content, English usage, format, citations, bibliographic style, and consistency, and is ready for submission to the College of Graduate Studies.

Richard D. Geer

Richard D Geer

11/8/96
Date

Approved for the Department of Chemistry

David M. Dooley

David M Dooley

11/8/96
Date

Approved for the College of Graduate Studies

Robert Brown

RL Brown

12/3/96
Date

STATEMENT OF PERMISSION TO USE

In presenting this thesis in partial fulfillment of the requirements for a doctoral degree at Montana State University-Bozeman, I agree that the Library shall make it available to borrowers under rules of the Library. I further agree that copying of this thesis is allowable only for scholarly purposes, consistent with "fair use" as prescribed in the U.S. Copyright Law. Requests for extensive copying or reproduction of this thesis should be referred to University Microfilms International, 300 North Zeeb Road, Ann Arbor, Michigan 48106, to whom I have granted "the exclusive right to reproduce and distribute my dissertation in and from microform along with the non-exclusive right to reproduce and distribute my abstract in any format in whole or in part."

Signature Wayne Harold Dickinson

Date 8 November 1996

TABLE OF CONTENTS

1.	PROBLEM STATEMENT AND RESEARCH OVERVIEW.....	1
	Microbially Influenced Corrosion.....	1
	Stainless Steel Corrosion.....	2
	Research Goal.....	3
	Overview of Research Leading to Elucidation of the Ennoblement Mechanism.....	4
2.	THE LITERATURE OF ENNOBLEMENT.....	5
	Ennoblement Characteristics.....	5
	Ennobled E_{corr}	7
	Elevated Cathodic Current.....	9
	Biological Origin.....	11
	Filtration and Other Control Measures.....	11
	Correlation with Indices of Biological Activity.....	13
	Mechanisms of Ennoblement.....	14
	Oxygen Reduction.....	14
	Other Cathodic Reactants.....	15
	Status of the Ennoblement Mechanism.....	16
	References Cited.....	18
3.	THEORY AND EXPERIMENTAL APPROACH.....	21
	Mixed Potential Theory.....	21
	Influence of Cathodic Rate on E_{corr}	22
	E_{corr} Measurements.....	27
	Potentiodynamic Polarization.....	28
	Redox Environment within Biofilms.....	29
	Microelectrode Measurements.....	30
	Oxygen Reduction Rate.....	31
	Surface Metal Oxide Abundance.....	31
	Capacitance Studies.....	33
	Coulometric Titration.....	34
	Metal-oxide Depositing Bacteria.....	35
	Anodic Polarization by Metal-Oxides.....	36
	Manganese-oxidizing Bacteria.....	37
	MOB and Manganese Deposition.....	38
	Reductive Dissolution of MnO_2	39
	Electrochemical Changes Induced by MnO_2	39
	Ennoblement by <i>Leptothrix discophora</i>	40
	Outline of the Thesis.....	41
	References Cited.....	42

4.	REDOX AND CAPACITANCE MEASUREMENTS	45
	Overview	45
	Introduction	46
	Experimental Procedure	48
	Results and Discussion	52
	Biofouling	52
	E _{corr} Measurements	53
	Microelectrode Studies	60
	Capacitance Studies	63
	Galvanostatic Reduction Measurements	71
	Conclusions	76
	References Cited	77
5.	ENNOBLEMENT BY MANGANIC OXIDE BIOFOULING	80
	Overview	80
	Introduction	81
	Experimental Methods	83
	In situ Exposure	83
	Biofilm Characterization	85
	MnO ₂ Studies	86
	Experimental Results	87
	Electrochemical Behavior	87
	Biofouling Deposits	91
	Sulfite Dissolution Experiment	95
	MnO ₂ Studies	97
	Discussion	99
	Mechanism of Ennoblement by MnO ₂	99
	Relationship to Previous Studies	101
	Ennoblement and Corrosion	103
	Conclusions	105
	References Cited	106
6.	MANGANESE DEPOSITION RATES	110
	Overview	110
	Introduction	111
	Experimental Methods	113
	Results	116
	Discussion	118
	Deposition Rates	118
	Model for Pit Formation	119
	Corrosion Rates	121
	Conclusions	121
	References Cited	123

7.	ENNOBLEMENT BY <i>LEPTOTHRIX DISCOPHORA</i>	126
	Overview	126
	Introduction	127
	Experimental	129
	Inoculum and Growth Medium	129
	Materials and Apparatus	130
	Experimental Procedure	131
	Analytical Methods	132
	Results and Discussion	134
	Bacterial Colonization	134
	Manganese Uptake and Deposition	136
	Effect of Bacteria and MnO _x on Ennoblement	137
	Relationship to Ennoblement in Natural Waters	140
	Conclusions	142
	References Cited	143
8.	SUMMARY AND CONCLUSIONS	147
	Overview	147
	Introduction	148
	MFOB and Localized Corrosion	149
	Stainless Steel Ennoblement	150
	Proposed Mechanism of Pit Formation by MFOB	154
	MnO ₂ Induced Corrosion	158
	Potential scope of MFOB Related corrosion	160
	MnO ₂ and SRB: Chemistry within the Deposits	162
	Nutrient Production	163
	Sulfide Removal	165
	Reactions with Corrosion Products	165
	Model for MFOB/SRB Induced Corrosion	167
	Concluding Remarks	168
	References Cited	170
	APPENDIX	174
	Galvanostatic pulse circuit and derivation of equation 3.20	174

LIST OF TABLES

Table 1.1. Schematic shift in E_{COR} with exposure time in natural and abiotic seawater.....	4
Table 5.1. Elemental composition of 316L SS coupons (as provided by vendor, Metal Samples Inc. Munford, AL.....	84
Table 7.1. Experimental approach to test the manganese biomineralization hypothesis	132

LIST OF FIGURES

Figure 2.1. Schematic shift in E_{corr} with exposure time in natural and abiotic seawater	6
Figure 2.2 Schematic diagram of cathodic polarization behavior before and after Ennoblement	6
Figure 3.1 Schematic diagram showing current-voltage relationships according to eq. 3.7 and 3.17. Curve 'P' illustrates behavior for a metal in the passive state. E_{corr} shifts from E_{corr}^1 to E_{corr}^2 as the equilibrium rate for the cathodic reaction increases.	27
Figure 4.1. E_{corr} for ten 316L stainless steel coupons during biofouling in fresh river water.	54
Figure 4.2. E_{corr} for four stainless steel control coupons during exposure to fresh river water. At times denoted by arrows, biofouling was removed from coupons by wiping surfaces with cotton.	55
Figure 4.3. E_{corr} for 10 stainless steel coupons after 35 day exposure to fresh river water, vs. E_{corr} after 10 hours exposure. Data from figure 4.1.	56
Figure 4.4. Potentiodynamic polarization curves for stainless steel before and after biofouling during 20 day exposure to fresh river water.	58
Figure 4.5. Microelectrode profiles in biofouling on Ennobled stainless steel coupons. Horizontal line indicates biofilm-solution interface: a) dissolved oxygen b) hydrogen peroxide c) E_{corr} for stainless steel probe.	61
Figure 4.6. Evolution of cathodic response to 10 nA cm^{-2} galvanostatic pulse as E_{corr} increases during biofouling of stainless steel in fresh river water. Data shown by solid lines, solid circles indicate points generated from curve fit to equation 4.1.	64
Figure 4.7. Capacitance and E_{corr} vs. time for two 316L stainless steel coupons during bifouling in fresh river water. (a) E_{corr} Ennobled during exposure (b) E_{corr} nearly constant during exposure.	66
Figure 4.8. Capacitance ratio vs E_{corr} for 6 stainless steel coupons during biofouling in fresh river water and for control coupon. $C(\text{init})$ is capacitance prior to exposure.	68
Figure 4.9. Polarization resistance and E_{corr} vs time for 316L stainless steel during biofouling in fresh river water.	71

- Figure 4.10. Galvanostatic reduction of 316L stainless steel in deaerated 0.1 M Na_2SO_4 , pH 8.5 for 4 coupons before and after 22 day exposure in fresh river water. $2.5 \mu\text{A cm}^{-2}$ applied current. 74
- Figure 4.11. Galvanostatic reduction behavior for two 316L stainless steel coupons in deaerated 0.1 M Na_2SO_4 , pH 8.5 after biofouling during 4 months exposure to fresh river water. $2.5 \mu\text{A cm}^{-2}$ applied current. 75
- Figure 5.1. E_{corr} vs. time for 316L stainless steel coupons during *in situ* exposure to fresh river-water. Data points for 3 coupons used for polarization measurements are shown, while shaded area envelopes curves for full 23 coupon set. At times denoted by arrows, cathodic polarization curves were measured. Horizontal dashed line indicates potential for MnO_2 coated coupon. 88
- Figure 5.2. Cathodic polarization curves for 316L SS coupons after different exposure intervals in fresh river-water, and for MnO_2 coated coupon. Measurements were made in air saturated 0.01M Na_2SO_4 / pH 8.4. 90
- Figure 5.3. Cathodic polarization curves in aerated and deaerated 0.01M Na_2SO_4 /pH 8.4 for 316L SS coupons after 500 hours *in situ* exposure to fresh river-water. 90
- Figure 5.4. SEM micrograph of annular deposits on SS coupon after 13 day *in situ* exposure to fresh river-water. SS substratum is visible within the central void. Arrow indicates site for EDS spectrum shown in figure 5.6. 93
- Figure 5.5. EDS maps of region shown in figure 5.4 confirming the presence of Mn, Ca, O, and C in the annular deposits. 93
- Figure 5.6. EDS spectrum for annular deposit on SS coupon at site designated by arrow in figure 5.4. Spectrum shows the presence of Mn and Ca which were undetectable at an adjacent site on the exposed substratum. 94
- Figure 5.7. Epifluorescence micrograph of acridine-orange stained biofilm on 316L SS coupon after 4 day *in situ* exposure to fresh river-water. Individual bacterial cells centrally located within a Mn-rich annular deposit (lower right) as well as sheathed filamentous bacteria can be seen. 94
- Figure 5.8. Influence of 0.5M SO_3^{2-} on E_{corr} for 316L SS after 20 day exposure to fresh river-water, and for unexposed coupon. Electrolyte was argon deaerated $0.5\text{M Na}_2\text{SO}_3 + 0.5\text{M Na}_2\text{SO}_4$, pH 8.4. Arrows denote time of sulfite addition. E_{corr} for a separate Ennobled coupon in deaerated 1M Na_2SO_4 , pH 8.4 is also shown. 95

- Figure 6.1. Micrographs of microbially colonized 316L stainless steel after 23 day exposure to fresh river water. (a) Epifluorescence image of acridine-orange stained biofilm showing distribution of cell clusters and presence of sheathed bacteria. (b) Reflected light image showing morphology and distribution of manganese-rich deposits..... 112
- Figure 6.2. Cathodic polarization curves for 316L stainless steel before and after formation of manganese-rich biofouling deposits..... 115
- Figure 6.3. Evolution of coulometric titration curves for 316L stainless steel with increasing duration of exposure to fresh river water. The curve for an MnO₂ paste coated coupon is also shown. 250 nA cm⁻² applied current in aerated 0.01 M Na₂SO₄ / pH 8.4..... 117
- Figure 6.4. Accumulation of cathodically active MnO₂ based on coulometric titration curves. Initial rate is 0.5 μg cm⁻² day⁻¹ for a one-electron reduction..... 117
- Figure 6.5. Model of stainless steel Ennoblement by microbially deposited MnO₂. E_{corr} shifts to the stability potential for MnO₂ reduction at experimental pH. For E_{corr} < E_{pit}, passivity is enhanced..... 119
- Figure 6.6. Conceptualized subsurface pit formation arising from microbial oxygen depletion within annular MnO₂ deposit. MnO₂ depolarization shifts E_{corr} to values exceeding E_{pit} at local sites of diminished redox potential..... 120
- Figure 7.1. Influence of Mn(II) on attached cell density for stainless steel coupons exposed to *Leptothrix discophora*. Initial Mn(II) = 200 μM..... 135
- Figure 7.2. Time dependence of soluble Mn(II) concentration and surface manganese abundance on stainless steel coupons. Surface manganese for an uninoculated control experiment was undetectable and is not shown..... 136
- Figure 7.3. Effect of *Leptothrix discophora* grown in media containing Mn(II) on E_{corr} for stainless steel..... 138
- Figure 7.4. Relationship between E_{corr}, surface manganese, and attached cell density for stainless steel coupons exposed to inoculated media containing Mn(II). 139
- Figure 8.1. E_{corr} vs. time for 316L stainless steel coupons during *in situ* exposure to fresh river-water. Data points for 3 coupons used for polarization measurements are shown, while shaded area envelopes curves for 23 coupon set. At times denoted by arrows, cathodic polarization curves were measured. Horizontal dashed line indicates potential for MnO₂-paste coated coupon..... 152

Figure 8.2. Cathodic polarization curves for 316L stainless steel coupons after different exposure intervals in fresh river-water, and for an unexposed coupon coated with MnO ₂ paste. Measurements were made in air saturated 0.01M Na ₂ SO ₄ / pH 8.4.	152
Figure 8.3. Galvanostatic reduction behavior for two 316L stainless steel coupons in deaerated 0.1 M Na ₂ SO ₄ / pH 8.5, after 4 months exposure to fresh river-water. 2.5 μA cm ⁻² applied current. E _{corr} values are at the end of the exposure period.	154
Figure 8.4. Reflected-light micrograph of annular deposits on 316L stainless steel coupon after 13 day <i>in situ</i> exposure to fresh river-water. Stainless steel substratum is visible outside the rings and within the central void.	157
Figure 8.5. Epifluorescence micrograph of acridine-orange stained biofilm on 316L stainless steel after exposure to fresh river-water. Individual bacterial cells centrally located within annular deposits as well as sheathed filamentous bacteria can be seen.	157
Figure 8.6. EDS maps of annular deposits on 316L stainless steel coupons confirming the presence of Mn, Ca, O, and C.	158
Figure 8.7. E _{corr} vs. time for MnO ₂ -paste coated 304L stainless steel coupon in 0.05N NaCl / pH 8.2. Polarization resistance at two points during exposure is shown.	159
Figure 8.8. Proposed model of corrosion processes within biomineralized MnO ₂ deposit containing SRB. MnO ₂ depolarization shifts E _{corr} to values exceeding E _{pit} at local sites of diminished redox potential. Cross-section through annular ring is shown.	168
Figure A.1. Equivalent circuit for constant current applied to an electrode-solution interface.	175
Figure A.2. Galvanostatic circuit used to assess capacitance according to equation 3.20.	178

NOTATION

i_{meas}	= measurable current, the sum of anodic and cathodic currents for all half-reactions
i_{net}	= the sum of anodic and cathodic currents for a single half-reaction
i_a	= anodic current
i_c	= cathodic current
i_{corr}	= corrosion current
i_o	= exchange current
i_{pass}	= passivation current
k^o	= standard rate constant for electrode reactions; (cm sec^{-1})
k_c^o	= standard rate constant for cathodic electrode reaction
k_a^o	= standard rate constant for anodic electrode reaction
n_a	= number of electrons transferred in rate determining step
n	= number of electrons transferred in net reaction
A	= electrode area; (cm^2)
C	= capacitance; (coul volt^{-1})
C_{ox}^*	= concentration of oxidized specie at the electrode surface; (moles cm^{-3})
C_{red}^*	= concentration of reduced specie at the electrode surface
C_c^*	= concentration of cathodic reactant at the electrode surface
C_a^*	= concentration of anodic reactant at the electrode surface
DO	= dissolved oxygen
E	= electrode potential
$E^{o'}$	= formal half-cell potential
$E_c^{o'}$	= formal half-cell potential for cathodic reactant
$E_a^{o'}$	= formal half-cell potential for anodic reactant
E_{corr}	= equilibrium electrode mixed potential
F	= Faraday constant, 96485 coulombs equivalent ⁻¹
I_{app}	= externally applied current

M	= molecular weight
MOB	= manganese-oxidizing bacteria
MFOB	= manganese- and iron-oxidizing bacteria
Q	= charge; (coulombs)
R	= gas constant; (8.31414 volt-coulombs mole ⁻¹ -deg ⁻¹ (K))
R _p	= polarization resistance; (ohm cm ²)
SS	= stainless steel
SCE	= saturated calomel electrode
SRB	= sulfate-reducing bacteria
T	= temperature; (degrees, K)
α _a	= anodic transfer coefficient
α _c	= cathodic transfer coefficient
β _a	= anodic Tafel slope; (Volts per decade of current)
β _c	= cathodic Tafel slope; (Volts per decade of current)
γ	= roughness factor
ρ	= density; (g cm ⁻³)

ABSTRACT

Microbial colonization of stainless steel (SS) surfaces can modify the electrochemical properties of the metal and increase the risk of corrosion damage. Two dominant effects of colonization -a several hundred millivolt noble shift in electrical potential and a two to three decade increase in cathodic current density- are implicated in the corrosion processes. These effects, collectively known as Ennoblement, are attributed to the metabolic activity of attached microorganisms, however the mechanism by which microbial activity modifies cathodic reactions at the metal surface remains unclear. The present dissertation investigates the role of microbially generated oxidants in Ennoblement and demonstrates that Ennoblement is caused by manganic oxide biomineralization.

Microelectrode measurements of dissolved oxidants within biofilms on SS indicated that redox potential in the bulk biofilm did not change during Ennoblement. A proposed mechanism involving oxygen electroreduction was also eliminated by showing that cathodic rates were independent of oxygen concentration. The findings directed attention to microbial production of surface-bound oxidants. Quantification of metal capacitance and surface-bound reactants suggested that metal oxides were involved in Ennoblement and led to the hypothesis that Ennoblement is caused by manganic oxide biodeposition.

Epifluorescence microscopy and bacterial culture methods confirmed the presence of manganese-oxidizing bacteria on Ennobled SS. Manganese-rich surface deposits were confirmed by wet chemical and energy-dispersive x-ray analysis. SS coated with MnO_2 paste exhibited electrochemical properties that closely matched those of Ennobled SS and elevated electrical potential decayed to pre-exposure values when bisulfite ion was used to reductively dissolve the surface manganese deposits. The biological mechanism of Ennoblement was validated by inducing the effect using pure cultures of the manganese-oxidizing bacterium *Leptothrix discophora*. Coulometric titration and wet chemical analysis demonstrated that 15-75 nmoles cm^{-2} of manganic oxide surface deposit shifts the potential of SS to a value near +350 mV versus the saturated calomel electrode.

Manganese-oxidizing bacteria have been widely reported at sites of SS corrosion. The present dissertation unifies this observation with the separate issue of Ennoblement by linking both issues to a common cause, manganic oxide biomineralization. The finding provides a plausible explanation for the corrosive effects of manganese-oxidizing bacteria on SS.

CHAPTER 1

PROBLEM STATEMENT AND RESEARCH OVERVIEW

Microbially Influenced Corrosion

Microbial colonization of metal surfaces can accelerate the corrosion of a variety of metals and metal alloys including aluminum, copper, nickel, iron, and steel. This effect, known as microbially-influenced corrosion (MIC), is widely implicated in the failure of metals exposed to aqueous systems and is the focus of worldwide research efforts. Such studies link MIC to the metabolic activities of microorganisms that modify the electrochemical environment near the metal surface; however, the complex chemistry of corrosion in the presence of microorganisms has made identification of exact mechanisms difficult. At present, the true nature of MIC is poorly understood.

One of the most puzzling aspects of MIC is the change in electrochemical properties of stainless steel that occurs as the metal surface is colonized by microorganisms. Microbial colonization in natural waters causes the corrosion potential (E_{corr}) of stainless steel to shift several-hundred millivolts in the positive or noble direction and produces an accompanying two to three decade increase in cathodic current density. These phenomena, collectively known as Ennoblement, increase the risk of localized corrosion of the metal. Concern over accelerated

stainless steel corrosion has stimulated research on Ennoblement for more than three decades, and has led to a thorough characterization of the phenomenon; nevertheless, no progress in establishing the mechanism of Ennoblement has been made.

Stainless Steel Corrosion

Stainless steel provides the corrosion resistance, strength, and temperature stability required for use in a variety of harsh environments. Typical applications include boiler and condenser tubing, containment vessels, and fluid pumps used in the steam electric, water and wastewater, food processing, and pulp and paper industries. Resistance to corrosion is imparted by formation of a thin surface oxide layer, or passive film, that inhibits the rate of metal dissolution. Oxidation of the principal alloying elements of stainless steel -iron, chromium, and nickel- is thermodynamically favored in aqueous media, and as a consequence, the protective passive film must be cohesive and contiguous to prevent sites of localized corrosion from developing.

Passive film breakdown can occur when elevated metal potential raises the metal-solution potential difference above an empirical value known as the critical pitting potential, E_{pit} . As damage to the oxide layer develops, oxidation and hydrolysis of the underlying metal can occur, producing an acidic environment and causing migration of charge-neutralizing counter ions to the metal surface. Surface acidification and counter-anion accumulation combine to prevent the protective oxide layer from reforming and generate an autocatalytic condition in which corrosion products stabilize the site of metal dissolution.

Rapid penetration of the metal can result, leading to perforation failures and costly repair or replacement of stainless steel tubing and containment vessels. Industries affected by this type of failure include the steam-electric power utilities, pulp and paper mills, petrochemical plants, wastewater-treatment facilities and the maritime industry.

In dilute chloride media, the positive shift in potential that develops during Ennoblement can exceed E_{pit} , enhancing the frequency of pit nucleation. Elevated current density supports the high local corrosion rate required to acidify and stabilize the nucleated site. Thus the two principal characteristics of Ennoblement, elevated E_{corr} and elevated current density, work in concert to aggravate the risk of localized corrosion and perforation failure of stainless steel.

Microbial activities that enhance the oxidizing power of the environment near the metal surface can be expected to elevate both E_{corr} and cathodic current density. Oxidizing power may increase due to microbial production of oxidizing chemicals, including both dissolved and solid-phase constituents, or due to acceleration of principal cathodic reactions, such as the reduction of dissolved oxygen, that occur even in the absence of microorganisms. Investigation of the role these factors play in Ennoblement is the primary research focus of this thesis.

Research Goal

The goal of the present research is to establish the mechanism by which microbial colonization induces the electrochemical phenomenon of Ennoblement. Table 1.1 provides an overview of the research objectives that were developed to achieve this goal.

Table 1.1 Overview of Research Leading to Elucidation of the Ennoblement Mechanism

Working Hypothesis	Experimental Approach	Outcome	Chapter
Ennoblement is caused by dissolved oxidants	Measure concentrations of specific oxidants (H_2O_2 , dissolved oxygen) and local E_{corr} within biofilms on Ennobled stainless steel	Dissolved oxidants do not cause Ennoblement	4
Ennoblement is caused by acceleration of the oxygen reduction reaction	Measure cathodic reaction rate for Ennobled stainless steel in the presence and absence of dissolved oxygen	Ennoblement is not caused by acceleration of the oxygen reduction reaction	5
Metal surface properties change during Ennoblement	Measure metal capacitance as a broad indicator of electrical double-layer and surface film properties	Ennoblement is correlated with changes in metal capacitance	4
The abundance of reducible surface-bound material increases during Ennoblement	Electrochemically titrate reducible surface material	A new oxidizing surface phase develops during Ennoblement	4 & 6
Ennoblement is caused by manganic oxide biofouling	1) Analyze biofilms for Mn-rich deposits and manganese-oxidizing bacteria. 2) Measure E_{corr} as Mn-rich deposits are chemically dissolved from the surface 3) Compare electrochemical characteristics of Ennoblement with those of stainless steel coated with pure MnO_2 paste	Manganic oxide mineralization causes Ennoblement	5
Ennoblement is caused by the activity of manganese-oxidizing bacteria	Assess Ennoblement of stainless steel exposed to pure cultures of <i>Leptothrix discophora</i>	Manganese-oxidizing bacteria can induce Ennoblement	7

CHAPTER 2

THE LITERATURE OF ENNOBLEMENT

Ennoblement Characteristics

The electrochemical phenomenon known as Ennoblement, was first observed in the mid-1960's¹, and has remained a controversial issue for the past three decades. The dominant characteristics of Ennoblement are a several-hundred millivolt increase in E_{corr} to values near +350 mV versus the saturated calomel electrode (SCE) and a two to three decade increase in cathodic current density at potentials between approximately -300 and +300 mV_{SCE}. These two defining electrochemical characteristics are depicted in figures 2.1 and 2.2. Studies have confirmed both effects for a variety of inert or passive metals including stainless steel, titanium, and platinum exposed to marine, estuarine, and fresh waters worldwide and have sought to demonstrate the biological nature of the phenomenon by showing that the shift in E_{corr} correlates with biofilm formation. A variety of mechanisms have been suggested to explain Ennoblement, but none has been supported by convincing experimental evidence.

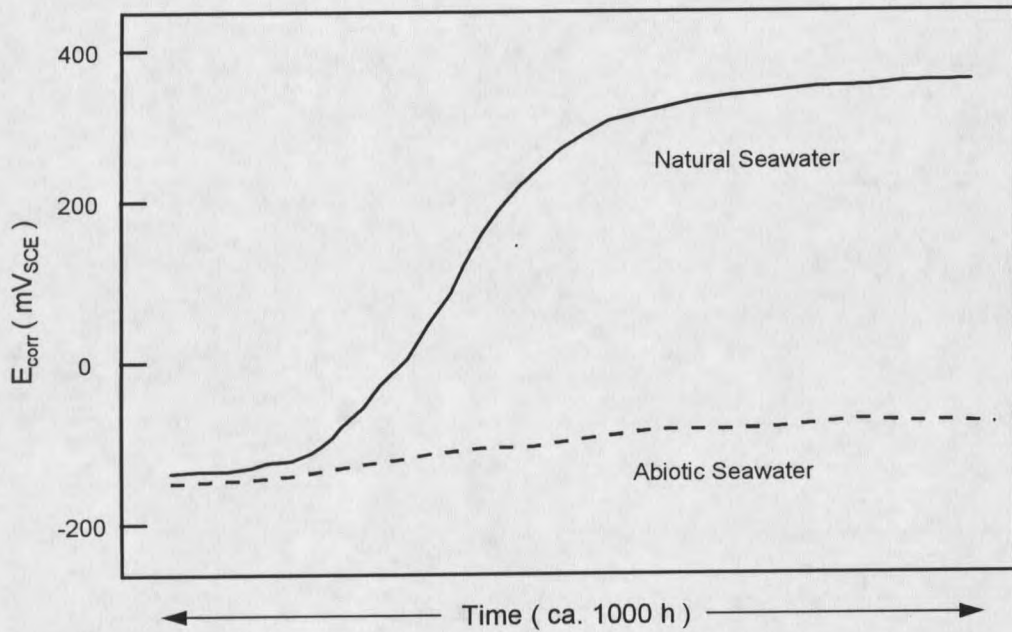


Figure 2.1. Schematic shift in E_{corr} with exposure time in natural and abiotic seawater

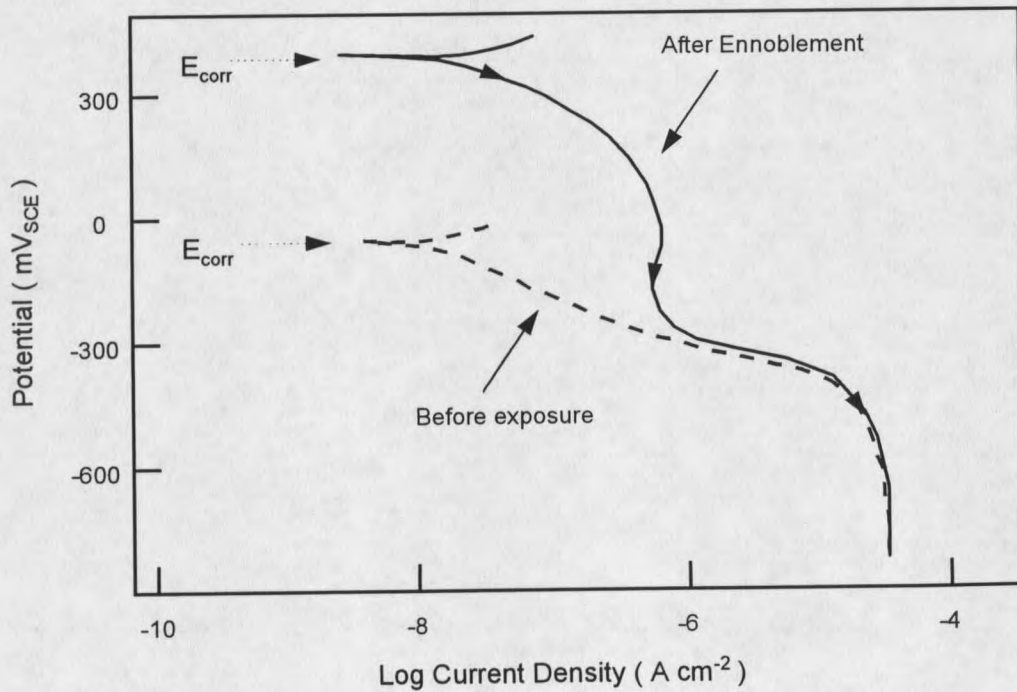


Figure 2.2 Schematic diagram of cathodic polarization behavior before and after Ennoblement

Ennobled E_{corr}

On initial exposure to seawater, E_{corr} for passive metals such as stainless steel and titanium lies in the range $-200 \text{ mV}_{\text{SCE}} < E_{\text{corr}} < -50 \text{ mV}_{\text{SCE}}$ ². Within a few days of exposure, E_{corr} typically begins to shift in the positive or noble direction reaching steady-state values between $+300$ and $+400 \text{ mV}_{\text{SCE}}$ within a few weeks. This shift is a defining characteristic of Ennoblement. Scotto et al.³ observed an initial increase in E_{corr} of approximately 20 mV d^{-1} for 22 Cr - 3 Mo - 0.6 Ti (wt. %) steel beginning within one day of exposure to seawater and increasing asymptotically towards $+375 \text{ mV}_{\text{SCE}}$ over 65 days. Mollica⁴ observed similar rates of increase towards the same limiting potential for a 17.5 Cr - 2.4 Mo - 0.6 Ti steel exposed to seawater, however the increase began only after ten days of exposure. Motoda et al.⁵ reported that E_{corr} reached $+400 \text{ mV}_{\text{SCE}}$ within 10 days for 18 different stainless alloys exposed to seawater near Shizuoka, Japan, and that E_{corr} for commercially pure Ti reached $+350 \text{ mV}_{\text{SCE}}$ during the same exposure. Chandrasekaran and Dexter⁶ found that E_{corr} for platinum became fixed at a value of $+400 \text{ mV}_{\text{SCE}}$ after 12 days exposure to saline water from the Delaware Bay near Lewes, DE. Dexter and Zhang⁷ reported E_{corr} values slightly over $+400 \text{ mV}_{\text{SCE}}$ for a series of stainless steels with molybdenum content between 0.2 and 6 wt % after 3 to 6 weeks exposure to fresh-water from a lake in Lewes, DE. Steady-state E_{corr} for replicate Ti samples varied between $+200$ and $+400 \text{ mV}_{\text{SCE}}$ during the same exposure. A collaboration of six European research centers⁸ confirmed steady-state E_{corr} of $+320 \text{ mV}_{\text{SCE}}$ for 24 Cr - 22 Ni - 7 Mo stainless steel exposed at coastal sites in the Norwegian sea, North sea, Mediterranean sea, and Eastern Atlantic. Time to reach steady-state varied from 6 to 19 days at the different

sites. Holthe et al.⁹ reported E_{corr} of +300 mV_{SCE} for Pt and 24 Cr - 22 Ni - 7 Mo stainless steel and E_{corr} of +260 mV_{SCE} for Ti after 30 days exposure to water from the Norwegian sea, however, E_{corr} for a 90 Cu - 10 Ni alloy remained nearly unchanged at -240 +/-30 mV_{SCE} during the same exposure.

Clearly, a noble shift in E_{corr} can occur for a variety of passive metals exposed to natural waters. Nevertheless, some authors^{10,11} have found that E_{corr} changes little during exposure, indicating that the effect is not universal. As an example, E_{corr} for stainless steel and titanium coupons remained less than +50 mV_{SCE} throughout a 4 month exposure to eastern coastal Pacific Ocean water¹⁰, and three types of stainless steel exposed to seawater from the Gulf of Mexico under continuous illumination showed steady-state E_{corr} of only +125 mV_{SCE}, less than 70 mV higher than E_{corr} for sterile controls¹¹. In the latter study, samples exposed under exclusively dark conditions showed a brief (1-2 day) noble excursion of E_{corr} , followed by a decay to a constant value of -100 mV_{SCE}. Anaerobic conditions were confirmed near the metal surface for this exposure, while dissolved oxygen levels of 2-3 ppm persisted at the surface for samples exposed under illuminated conditions. Results of this study suggested that anaerobic conditions are inconsistent with Ennoblement.

The foregoing indicates that metals with very low corrosion currents such as stainless steel, platinum, and titanium can attain E_{corr} values between +300 and +400 mV_{SCE} during exposure to waters at diverse geographic locations. This limiting range, independent of metal composition, implies that E_{corr} is influenced by processes external to the metal rather than by changes in the metallurgy that occur during exposure. The similarity in steady-state E_{corr} for different locations suggests that a common process is occurring at the different sites, although

the rate of development of the process appears to vary with location. The failure of the Cu-Ni alloy to become Ennobled may indicate that corrosion current is an important factor since Cu-Ni has a considerably higher corrosion rate than the other metals⁹. This explanation is consistent with the fact that Ennoblement has never been reported for mild steel or other actively corroding metals. A relationship between corrosion current and Ennoblement could reflect a balance between the rate of formation of a new oxidizing chemical specie and the rate of discharge of this specie through the corrosion current.

Elevated Cathodic Current

A second defining electrochemical characteristic that develops for passive metals exposed to natural waters is an increase in cathodic current density (i_c). A shift toward greater cathodic current indicates an increase in the rate at which reduction reactions occur at the metal surface. Mollica⁴, investigating the electrochemical behavior of 17.5 Cr - 2.4 Mo - 0.6 Ti steel in seawater, observed an increase in i_c over the potential range -250 to +300 mV_{SCE}. After 30 days exposure, i_c had increased by 0.8 decades at -200 mV_{SCE} and 3.2 decades at +250 mV_{SCE}. Below -250 mV_{SCE} the current before and after exposure was identical. Motoda et al.⁵ observed an increase in i_c over exactly the same potential range for type 316 stainless steel. After 14 days exposure to seawater, i_c had increased by 2 decades at +300 mV. Unlike Mollica's findings, however, where i_c increased steadily with decreasing potential, the increase in i_c showed a maximum of 2.3 decades at 0 mV_{SCE} for Motoda's work. Ijsseling¹² examined the cathodic behavior of a 24 Cr - 22 Ni - 7 Mo stainless steel in seawater for

exposure periods up to 160 days. Cathodic current density increased over the same range of potentials as noted above. The increase at $-200 \text{ mV}_{\text{SCE}}$ varied from 0.8 decades after 15 days to 1.2 decades after 133 days. At $+250 \text{ mV}_{\text{SCE}}$, the increase was 2.2 decades after 15 days and 3.0 decades after 133 days. Ijsseling also examined the influence of polarization scan rate (0.9 , 0.09 , and 0.009 mV s^{-1}) on cathodic current. Throughout the range $+250$ to $-200 \text{ mV}_{\text{SCE}}$, i_c increased with increasing scan rate and was 3 to 8 times greater at a scan rate of 0.9 mV s^{-1} than at a rate of 0.009 mV s^{-1} . A well resolved maximum occurred in the $\log i_c$ vs. potential (E) curves at $0 \text{ mV}_{\text{SCE}}$ and $-200 \text{ mV}_{\text{SCE}}$ for the 0.09 and 0.9 mV s^{-1} sweep rates respectively. Only a very slight maximum at $+140 \text{ mV}_{\text{SCE}}$ was identifiable for the 0.009 mV s^{-1} sweep. At 0.009 mV s^{-1} , i_c at $-600 \text{ mV}_{\text{SCE}}$ was $20 \mu\text{A cm}^{-2}$ before and after 150 days exposure. In contrast after 150 days, i_c at $-600 \text{ mV}_{\text{SCE}}$ was 70 and $130 \mu\text{A cm}^{-2}$ for scan rates of 0.09 and 0.9 mV s^{-1} respectively.

It is apparent that i_c increases up to 2-3 decades in the potential range -250 to $+300 \text{ mV}_{\text{SCE}}$ for stainless alloys exposed to seawater. A maximum in the $\log i_c$ vs. E curves also develops, and this may indicate that a mass transfer limitation or depletion of a reducible specie occurs during the scan. The former could occur if a new electrode process decreases the oxygen reduction overvoltage, whereas the latter condition would result if a finite amount of a new reducible specie is formed near the electrode surface since cathodic current furnished by this specie would decrease as the specie becomes depleted by reduction. Either of these possibilities could explain the increase in cathodic current density observed during Ennoblement, and both are consistent with the scan rate dependence of i_c that was observed

(i.e. i_c may be higher at faster scan rates due to less depletion of the new reducible specie or due to establishment of a smaller diffusion field).

Biological Origin

Several approaches have been used to determine if Ennoblement is caused by microbial colonization of the metal surface. These can be roughly classified as controlled biotic experiments and experiments designed to correlate Ennoblement with biological parameters such as biomass and respiratory activity.

Filtration and Other Control Measures

The effect of filtration and pasteurization on the development of Ennoblement was investigated by Dexter^{7,13} for a variety of stainless alloys exposed to seawater and to estuarine waters from the Delaware Bay. Control experiments were carried out by exposing the alloys to the same waters treated by low temperature pasteurization (75°C) and filtration through 0.2 μm membranes. Ennobled E_{corr} and a 30-160 μm thick biofilm developed within 20 days for coupons exposed to untreated water, while E_{corr} remained less than 0 mV_{SCE} and negligible biofilm developed for the control coupons. Scotto³ observed similar results for control experiments involving only filter sterilization. Johnsen and Bardal¹⁴ compared E_{corr} for stainless steel exposed to natural seawater and to abiotic synthetic seawater. E_{corr} increased to +300 mV_{SCE} after 12 days exposure to seawater and remained stable at that potential

throughout the ensuing 6 weeks of exposure. In contrast, E_{corr} did not exceed +130 mV_{SCE} for the coupon exposed to synthetic seawater. These studies demonstrated a correlation between Ennoblement and attached bacterial cell density, however, neither filtration nor filtration plus pasteurization produced entirely abiotic controls. As a consequence, a purely biological basis for Ennoblement could not be inferred.

Mollica⁴ investigated the effect of flow rate on Ennoblement. The rate of increase in E_{corr} shifted from 20 to 7 mV d⁻¹ as flow rate was increased from 1 to 5 m s⁻¹. It was shown that the rate of increase in E_{corr} correlated with dried weight of biofilm on the metal surface, and that the biofilm mass decreased with increasing flow rate.

Holthe et al.⁹ investigated the relationship between Ennoblement and temperature by exposing stainless steel to seawater in a heated recirculation loop. For temperatures less than 32°C, E_{corr} shifted to +300 mV_{SCE} during a 24 day exposure. At 32°C, E_{corr} remained less than +100 mV_{SCE} throughout the exposure. Mollica¹⁵ found a similar effect with a transition temperature of 35-40 °C, above which Ennoblement did not occur. The results were attributed to a decrease in microbial viability at the higher temperatures as indicated by a low ATP content in the surface deposits formed at temperatures greater than 35°C. A relationship between cathodic current and temperature was observed for stainless steels exposed to seawater in the Mediterranean, eastern coastal Atlantic, and North Sea⁸. The exposure time required for elevated cathodic current to develop decreased with increasing water temperature over the range 2 - 21°C. The correlation is consistent with the temperature dependence of biological growth although the effect of other seasonal and chemical parameters on the rate of cathodic current increase could not be evaluated.

Correlation with Indices of Biological Activity

Scotto et al.¹⁶ compared E_{corr} with the respiratory activity of biofilms -measured as oxygen uptake- on a 20 Cr - 18 Ni - 6 Mo stainless steel exposed to seawater. E_{corr} covaried with the logarithm of respiratory activity. E_{corr} and cathodic current density also correlated with the logarithm of the amount of extracellular polymeric substances (EPS) -measured as polysaccharide content- in the biofilms. The onset of increased cathodic current occurred when approximately 150 ng cm^{-2} of EPS had been deposited on the coupon surface. In a related experiment³, the same authors showed that attached bacterial cell density and E_{corr} evolved towards limiting values according to an equation of the form

$$X = X_{\infty} (1 - e^{-kt})$$

Where X is the value at time, t , X_{∞} is the value at infinite time and k is a constant with the empirical value $2.5 \times 10^{-2} \text{ d}^{-1}$. Mollica¹⁵ observed that Ennobled E_{corr} developed only when the ATP content in the biofilm was greater than approximately 1 ng cm^{-2} . Gundersen et al.¹⁷ investigated the effect of hypochlorite on Ennoblement, using a lipid hydrolysis technique to assess bacterial activity. Hypochlorite applied at 1 ppm for 30 minutes daily was effective in eliminating bioactivity and prevented Ennoblement from developing.

Another study of the biological nature of Ennoblement used sodium azide to poison biofilms on Ennobled metals³. Azide addition caused E_{corr} for a stainless alloy to drop from +375 to +125 mV_{SCE} over a five day period. Dexter¹³ observed similar effects for Ennobled platinum. Since azide inhibits respiration without causing biofilm detachment, it was concluded that active metabolism rather than the mere physical presence of the biofilm was

responsible for Ennoblement. Dexter pointed out, however, that azide produces a significant drop in E_{corr} even for abiotic controls, although the magnitude of such decrease is much smaller than that observed for the azide treatment of Ennobled samples.

Mechanisms of Ennoblement

Oxygen Reduction

Oxygen reduction is the dominant cathodic reaction on stainless steel under aerated conditions, and much attention has been focused on the relationship between oxygen reduction and Ennoblement.

Oxygen concentration can be influenced by photosynthetic activity within biofilms and this consideration has been used to interpret data from Ennoblement experiments. Little¹¹ attributed the absence of Ennoblement for coupons exposed under dark conditions to a lack of photosynthesis that allowed anaerobic conditions to develop. Motoda⁵ found high numbers of attached diatoms on Ennobled stainless steel and argued that Ennoblement was caused by a metabolite of the diatoms. Scotto¹⁶ however, found no correlation between Ennoblement and chlorophyll-a content in the biofilms and Mollica¹⁵ observed that Ennoblement occurred even when chlorophyll-a was negligible. Dexter⁷ found that sunlight had a deleterious effect on the development of Ennoblement, and argued that this was caused by a decrease in the thermodynamic potential for oxygen reduction brought about by algal consumption of CO_2 that increased pH near the metal surface. Eashwar et al.¹⁸ reported that exposure to direct

sunlight prevented Ennoblement from occurring in waters that otherwise caused a 250 mV increase in E_{corr} .

Many authors have suggested that acceleration of the oxygen reduction reaction -possibly by metallo-organic catalysts produced during microbial respiration- is the cause of Ennoblement^{15,16,19}. This idea has become quite well entrenched, although no direct evidence of accelerated oxygen reduction has been presented. As indicated by studies on the effects of photosynthesis, a coherent picture of the role of oxygen in Ennoblement is missing.

Other Cathodic Reactants

Dexter¹³ attribute the finding that Ennobled E_{corr} decreased during daylight hours to an increase in pH, implying that Ennoblement was associated with acidification at the metal surface. Protons are a dominant cathodic reactant in deaerated media and in aerated media, pH causes a thermodynamic shift in the oxygen reduction potential of -60 mV pH^{-1} . Thus a pH drop of 5-6 units from a seawater pH near 8.0 could explain Ennoblement. Dexter suggested that pH 3 could be reached within biofilms containing acid producing bacteria and Chandrasekaran and Dexter⁶ argued that at pH 3, 8 mM hydrogen peroxide could account for the electrochemical characteristics of Ennobled platinum. Their conclusion was based in part on detection of several mM hydrogen peroxide in the biofilm. Mollica²⁰ however, found that seawater acidified to pH 7.5 caused little change in E_{corr} while the same seawater left untreated caused E_{corr} to shift to $+300 \text{ mV}_{\text{SCE}}$. From this and other data, he concluded that Ennoblement was prevented by acidification. Mansfeld et al.¹⁰ pointed out that acidification lowers the

pitting potential of low molybdenum stainless steels below the value of Ennobled E_{corr} , thus making Ennoblement and acidification mutually exclusive.

Status of the Ennoblement Mechanism

Although several hypotheses have been suggested, most investigators acknowledge that the mechanism underlying Ennoblement remains unexplained^{5,9,10,13,16,18,21}. Research undertaken in the present thesis was designed to establish the mechanism of Ennoblement, and was initiated by testing several of the Ennoblement hypotheses. Careful analysis and interpretation of the results of these experiments led to a new hypothesis involving manganese-oxidizing bacteria and to the confirmation of this hypothesis. The following paragraph briefly summarizes how this finding fits into previous knowledge concerning manganese-oxidizing bacteria and corrosion.

The occurrence of manganese and manganese-oxidizing bacteria at sites of stainless steel corrosion has been widely observed and is commonly thought to result from differential aeration caused by mineral occlusion of the metal surface²²⁻²⁵. Several authors^{23,26,27} have noted, however, that microbial production of ferric and manganic chlorides would be corrosive to stainless steel, and Duquette and Ricker²⁸ suggested that these species would act to fix the metal potential above the pitting potential. Linhardt²⁹ demonstrated that manganese containing deposits from a severely pitted stainless steel turbine blade, when applied to a platinum electrode, could shift the metal potential above +300 mV_{SCE}. This potential was above the stainless steel pitting potential for water of approximately 100 ppm chloride, and

was thought to be the cause of the corrosion failure. These observations taken together with a mechanism of Ennoblement involving manganese-oxidizing bacteria, serve to unify the previously separate issues of Ennoblement and manganese-related corrosion by linking them to a common cause, biomineralization of manganese dioxide. Direct electrochemical reduction of the manganese dioxide, operating independently or in conjunction with surface occlusion processes, appears to be a significant factor in the corrosion mechanism.

References Cited

1. Crolet, J.-L. (1991). From Biology and Corrosion to Biocorrosion, in: Microbial Corrosion: Proceedings of the 2nd EFC Workshop. Sequeira, C.A.C., and A. K. Tiller eds., (Sesimbra, Portugal, 3-6 March 1991, The Institute of Materials, London), pp. 50-60.
2. Lula, R. (1986). Stainless Steel. (American Society of Metals, Metals Park, OH), 173 pp.
3. Scotto, V., R. DiCintio and G. Marcenaro, (1985). The Influence of Marine Aerobic Microbial Film on Stainless Steel Corrosion Behaviour. *Corr. Sci.* **25**:185-194.
4. Mollica, A. (1976). The Influence of the Microbiological Film on Stainless Steels in Natural Seawater, in: The 4th International Congress on Marine Corrosion and Fouling (Antibes, France), pp. 351-365.
5. Motoda, S., Y. Suzuki, T. Shinohara and S. Tsujikawa, (1990). The Effect of Marine Fouling on the Ennoblement of Electrode Potential for Stainless Steels. *Corr. Sci.* **31**:515-520.
6. Chandrasekaran, P. and S. C. Dexter, (1993). Mechanism of Potential Ennoblement on Passive Metals by Seawater Biofilms, CORROSION/93 paper no. 493 (NACE, Houston, TX).
7. Dexter, S. C. and H.-J. Zhang, (1990). Effect of Biofilms on Corrosion Potential of Stainless Steel Alloys in Estuarine Waters, in: The 11th International Corrosion Congress (Associazione Italiana di Metallurgia, Florence, Italy) pp. 333-340.
8. Audouard, J., *et al.*, (1994). Effect of Marine Biofilm on High Performance Stainless Steels Exposed in European Coastal Waters. in: The Third European Federation of Corrosion Workshop on Microbial Corrosion. Tiller, A.K. and C.A.C Sequeira, eds., (Estoril, Portugal, 13-16 March 1994, The Institute of Materials, London) pp. 198-210.
9. Holthe, R., E. Bardal and P. Gartland, (1989). Time Dependence of Cathodic Properties of Materials in Seawater. *Mat. Perform.* **28**:16-23.
10. Mansfeld, F., *et al.*, (1992). An Electrochemical and Surface Analytical Study of Stainless Steels and Titanium Exposed to Seawater. *Corr. Sci.* **33**:445-456.
11. Little, B.J., *et al.*, (1991). Impact of Biofouling on the Electrochemical Behaviour of 304 Stainless Steel in Natural Seawater. *Biofouling* **3**:45-49.

12. Ijsseling, F., (1993). Improved Method for Measuring Polarisation Curves of Alloys during Prolonged Times of Exposure. in: Marine Corrosion of Stainless Steels: Chlorination and Microbial Effects. Ijsseling, F.P., ed. (The Institute of Materials, London), pp. 100-107.
13. Dexter, S., (1995). Effect of Biofilms on Marine Corrosion of Passive Alloys. in: Bioextraction and Biodeterioration of Metals. Gaylarde, C. and H. Videla eds., (Cambridge University Press, Cambridge, UK); pp. 129-168.
14. Johnsen, R. and E. Bardal, (1986). Effect of a Microbiological Slime Layer on Stainless Steels in Seawater. CORROSION/86 paper no. 227 (NACE, Houston, TX).
15. Mollica, A., *et al.*, (1989). Cathodic Performance of Stainless Steels in Natural Seawater as a Function of Microorganism Settlement and Temperature. Corrosion **45**:48-56 .
16. Scotto, V., M. Beggiato, G. Marcenaro and R. Dellepiane, (1993). Microbial and Biochemical Factors Affecting the Corrosion Behaviour of Stainless Steels in Seawater. in: Marine Corrosion of Stainless Steels: Chlorination and Microbial Effects. Ijsseling, F.P., ed. (The Institute of Materials, London), pp. 21-33.
17. Gundersen, R., *et al.*, (1991). The Effect of Sodium Hypochlorite on the Electrochemical Properties of Stainless Steels in Seawater with and without Bacterial Films. Corrosion **47**:800-807.
18. Eashwar, M., S. Maruthamuthu, S. Palanichamy and K. Balakrishnan, (1995). Sunlight Irradiation of Seawater Eliminates Ennoblement-Causation by Biofilms. Biofouling **8**:215-221.
19. Dexter, S. C. and G. Y. Gao, (1988). Effect of Seawater Biofilms on Corrosion Potential and Oxygen Reduction of Stainless Steel. Corrosion **44**:717-723.
20. Mollica, A., (1992). Biofilm and Corrosion on Active-Passive Alloys in Seawater. Internat. Biodeterio. Biodegrad. **29**:213-229.
21. Dowling, N., J. Guezennec, J. Bullen, B. Little and D. White, (1992). Effect of Photosynthetic Biofilms on the Open-Circuit Potential of Stainless Steel. Biofouling **5**:315-322.
22. Tatnall, R.E., (1981). Case histories: Bacteria Induced Corrosion. Mat. Perform. **20**:41-48.
23. Kobrin, G., (1986). Reflections on Microbiologically Induced Corrosion of Stainless Steels. in: Biologically Induced Corrosion. Dexter, S. C. ed., (NACE, Houston, TX) pp. 33-46.

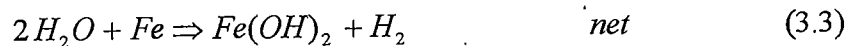
24. Tverberg, J., K. Pinnow and L. Redmerski, (1990). The Role of Manganese Fixing Bacteria on the Corrosion of Stainless Steel. CORROSION/90 paper no. 151 (NACE, Houston, TX).
25. Tuthill, A., R. Avery, J. Musich, K. Pinnow and R. Lutey, (1995). Corrosion of Stainless Steel Piping in a High Manganese Fresh Water. in: 1995 International Conference on Microbially Influenced Corrosion. Angell, P. *et al.* eds., (New Orleans, 8-10 May, 1995, NACE, Houston, TX), pp. 54/1-54/7.
26. Tatnall, R., (1990). Case Histories: Biocorrosion. in: Biofouling and Biocorrosion in Industrial Water Systems. Flemming, H-C. and G. Geesey, eds., (Springer-Verlag, New York) pp. 165-185.
27. Videla, H. A. and W.G. Characklis, (1992). Biofouling and Microbially Influenced Corrosion. *Internat. Biodeterio. Biodegrad.* **29**:195-207.
28. Duquette, D., and R. Ricker (1986). Electrochemical Aspects of Microbially Induced Corrosion. in: *Biologically Induced Corrosion*. Dexter, S.C. ed., (NACE, Houston, TX), pp. 121-130.
29. Linhardt, P., (1994). Manganese Oxidizing Bacteria and Pitting of Turbine Components Made of CrNi Steel in a Hydroelectric Power Plant. *Werkst. Korros.* **45**:79-83.

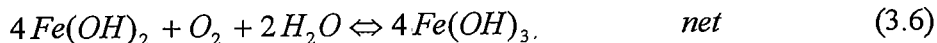
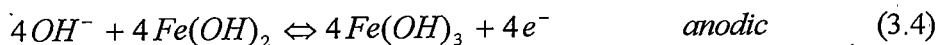
CHAPTER 3

THEORY AND EXPERIMENTAL APPROACH

Mixed Potential Theory

The potential of an electrode in solution reflects relative rates of anodic (oxidation) and cathodic (reduction) reactions occurring at the electrode surface. At equilibrium, the net rates of anodic and cathodic reactions are equal, and the electrode potential is constant. For inert or noble metals, such as platinum and gold, the electrode itself does not undergo reaction and serves only to facilitate charge transfer between external redox species. In contrast, electrodes of active metals such as iron do undergo oxidation and this process contributes to the net anodic rate. Metal oxidation is typically the dominant anodic process for freely corroding materials. In aerated solution, the dominant cathodic reactions are reduction of dissolved oxygen (DO) and reduction of water¹. Equations 3.1-3.6 show relevant half-reactions and the corresponding net reaction for the corrosion of iron in aerated aqueous media^{2,3}.





Eqs. 3.1-3.6 indicate that the anodic and cathodic processes occurring on the metal surface correspond to different half-reactions. The term 'mixed potential' is used to describe this condition, and to distinguish it from a reduction potential in which the anodic and cathodic reactions are simply the forward and reverse parts of a single half-reaction. A mixed-potential in which the anodic reaction is metal oxidation is termed the corrosion potential, E_{corr} .

Influence of Cathodic Rate on E_{corr}

The net rate for each half-reaction occurring on the metal surface is given by Butler-Volmer kinetics^{1,4} as:

$$i_{\text{net}} = nFAk^o \left\{ C_{\text{ox}}^* \exp \left[-2.3 \frac{(E - E^o)}{B_c} \right] - C_{\text{red}}^* \exp \left[2.3 \frac{(E - E^o)}{B_a} \right] \right\} \quad (3.7)$$

$$B_c = \frac{2.3 RT}{\alpha_c n_c F} \quad B_a = \frac{2.3 RT}{\alpha_a n_a F}$$

where cathodic and anodic rates for each half-reaction are described by the first and second exponential terms in eq. 3.7 respectively, E refers to the electrode potential, and C_{ox}^* and C_{red}^* refer to concentrations of the oxidized and reduced species at the electrode surface. Other symbols are as defined in the Notation section. Measureable current across the

electrode-solution interface is the sum of the net currents for each half-reaction and at equilibrium, must equal zero. For n separate half-reactions:

$$i_{meas} = \sum_{j=1}^n i_{net}^j \quad (3.8)$$

Bearing in mind that only a single value of E can exist for a conductive surface, and setting the sum of currents described by eq. 3.8 to zero, E can be expressed in terms of the reactant concentrations, formal half-cell potentials (E°), and kinetic parameters associated with each half-reaction. If as is often the case, the anodic and cathodic rates are dominated by single half-reactions (e.g. reactions 3.1 and 3.2), and further, if the intrinsic rates for these half-reactions under the concentration conditions of the system are similar, E will acquire a value intermediate between the standard potentials of the dominant anodic and cathodic reactions. Equation 3.7 shows that in so doing, the cathodic rate for half-reactions possessing a formal potential more positive than E , and the anodic rate for half-reactions possessing a formal potential more negative than E , will increase. At the same time, rates of the reverse reactions decrease. Expressed in another way, for $C_{ox}^* = C_{red}^*$ and $E \ll E^{\circ}$, the first exponential term in equation 3.7 dominates and the equation becomes:

$$i_c = nFAk_c^{\circ} C_c^* \exp \left[-2.3 \frac{(E - E_c^{\circ})}{B_c} \right] \quad (3.9)$$

Where i_{net} has been changed to i_c , to indicate that the net current for the half-reaction with the more positive reduction potential is cathodic. The subscript c has been added to indicate that this equation describes the current supplied by the cathodic half-reaction.

